2-1-1994

Solid H_2 and D_2: Remarkable Differences in Some NMR Properties

A. Brooks Harris
University of Pennsylvania, harris@sas.upenn.edu

Horst Meyer

X. Qin

Recommended Citation
Harris, A., Meyer, H., & Qin, X. (1994). Solid H_2 and D_2: Remarkable Differences in Some NMR Properties. *Physical Review B, 49* (6), 3844-3856. http://dx.doi.org/10.1103/PhysRevB.49.3844

Solid H_2 and D_2: Remarkable Differences in Some NMR Properties

Abstract
The differences in the observed properties of solid H_2 and D_2 are reviewed, and in particular those encountered in NMR experiments. The failure to detect a sharp NMR (I=1) impurity "isolated pair" spectrum in *p*-D2 is discussed in terms of a larger crystalline field than in H_2, where an intense and sharp pair spectrum has been observed. Furthermore, we discuss the dramatic (I=1) solid echo signal loss with decreasing temperature which is observed in solid D_2, but not for solid H_2. A theory of the solid echo damping through orientational fluctuations is developed. This theory accounts for the observed solid echo decay in D_2 as a function of the pulse spacing time τ and leads to an estimation of the order parameter fluctuation amplitude and the correlation time τ_c. However, the theory cannot account for the loss of spin (as determined from Curie's law), which must occur for very small values of τ that are not covered by the theory.

Disciplines
Physics | Quantum Physics

Solid H_2 and D_2: Remarkable differences in some NMR properties

A. B. Harris
Department of Physics, University of Pennsylvania, Philadelphia, Pennsylvania 19104-6396

H. Meyer and X. Qin
Department of Physics, Duke University, Durham, North Carolina, 27708-0305
(Received 3 September 1993)

The differences in the observed properties of solid H_2 and D_2 are reviewed, and in particular those encountered in NMR experiments. The failure to detect a sharp NMR ($I = 1$) impurity "isolated pair" spectrum in p-D_2 is discussed in terms of a larger crystalline field than in H_2, where an intense and sharp pair spectrum has been observed. Furthermore, we discuss the dramatic ($I = 1$) solid echo signal loss with decreasing temperature which is observed in solid D_2, but not for solid H_2. A theory of the solid echo damping through orientational fluctuations is developed. This theory accounts for the observed solid echo decay in D_2 as a function of the pulse spacing time τ and leads to an estimation of the order parameter fluctuation amplitude and the correlation time τ_c. However, the theory cannot account for the loss of spin (as determined from Curie's law), which must occur for very small values of τ that are not covered by the theory.

I. INTRODUCTION

Several experiments have shown remarkable differences in the behavior of solid H_2 and D_2. Some of these differences are fairly well understood, such as (A) the much slower rate of para-ortho conversion in D_2 as compared to that of orth-para conversion in H_2, and (B) the much slower quantum diffusion in D_2 as compared to that in H_2. For a review of these properties see Ref. 1.

Several other phenomena which show important differences between solid H_2 and D_2 need a better understanding. For instance, (C) the dynamics of the martensitic hcp⇔fcc transformation is quite different in D_2 as compared to H_2.[2] In particular, in solid D_2 (but not for solid H_2) repeated thermal cycling is found to stabilize the fcc phase at temperatures above that at which this phase is believed to be the thermodynamically stable one. Other puzzling differences between these two similar solids include (D) the fact that the impurity NMR spectrum of sharp lines from ($J = 1$) pairs has been observed in ($J = 0$) H_2 (Ref. 3) but not in D_2.[4] Also (E) at temperatures below 1 K where orientational ordering increases and a glassy state[5] gradually appears,[6] there is an anomalous loss of signal in the solid echo (of NMR) for D_2 but not for H_2.[7] A similar loss of echo signal has also been observed[8] from H_2 impurities in D_2 samples undergoing orientational ordering into a glassy state. In this paper we review briefly some aspects of these phenomena and discuss possible explanations of phenomena (D) and (E).

Of course, as far as most properties are concerned, solid H_2 and D_2 are quite similar.[1] For the present discussion we review briefly (F) orientational ordering, which can be explained by the dominance of electrostatic quadrupolar interactions in both solids.

First we briefly recapitulate some of the properties of these two solids that might be relevant in a discussion of the anomalies in the solid echo amplitude.

A. Ortho-para conversion

It has long been understood why the rate of species conversion (ortho→para in H_2, para→ortho in D_2) after cooling the solid sample is so much smaller in D_2 than in H_2. This process requires the spatially inhomogeneous part of the intermolecular dipolar interaction to simultaneously change both the nuclear spin parity and the rotational angular momentum. Detailed calculations[1] show that the conversion rate in D_2 is smaller than that in H_2 by a ratio r, which is of order $(\mu_D/\mu_H)^4$, where μ_D (μ_H) is the nuclear dipole moment of the deuteron (proton).

B. Quantum diffusion

As shown by van Kranendonk,[9] quantum diffusion results from resonant ortho-para conversion: one molecule changing its angular momentum J from 1 to 0, while one of its neighbors changes its J from 0 to 1, and the same dependence as above on r was obtained for this process. Thus r being much smaller than unity implies that quantum diffusion and the resulting clustering of ($J = 1$) molecules is much slower in D_2 than in H_2. Hence while clustering is easily observed in various experiments with H_2, where it has a substantial effect on various properties such as the NMR signal (for a review see Ref. 10), evidence of very slow clustering has been detected in solid D_2.[11]

C. Dynamics of the martensitic transition

Both H_2 and D_2 grow in the hcp phase. Near 4 K at zero pressure their molar volumes are[1] respectively 23.15

and 19.95 cm^3/mol, the differences being attributable to the larger zero-point vibration amplitude in H_2. Upon the transition into the long-range orientationally ordered state, the cubic crystalline phase with the four sublattice $Pa3$ structure becomes stabilized. The martensitic transition dynamics between the hcp and the cubic phases upon changing from the ordered into the disordered phase is quite different for H_2 and D_2 and has been discussed elsewhere.[2] In particular, for D_2 (but not for H_2) repeated thermal cycling leads to the metastable existence of the fcc phase at temperatures above the orientational ordering temperature. Initially,[12] it seemed natural to try to relate this result to the difference in density or the difference in the zero-point motion of the two solids. However, later experiments[2] showed that solid H_2 pressurized to have the same density as solid D_2 at zero pressures is still quite similar to solid H_2 at zero pressure. Since the amplitude of the zero-point motion decreases as the pressure is increased, an explanation in terms of the density or zero-point motion does not explain the more recent experiments[2] under pressure. Thus, this phenomenon lacks a satisfactory explanation. An explanation in terms of nucleation dynamics and domain-wall energies has not yet been made, and it is hoped that future research can be undertaken in this direction.

D. NMR spectra of nearest neighbor ($J = 1$) pairs

In a nearly pure ($J = 0$) crystal of the hydrogens it is possible to observe the NMR signal from a small (of order a few percent or less) concentration X of ($J = 1$) molecules. If these molecules are distributed randomly, the fraction of them which form isolated pairs of nearest neighboring ($J = 1$) molecules, N_p/N, is then $N_p/N = 12X(1 - X)$[18]. However, in solid H_2 the o-H_2 molecules are mobile (due to quantum diffusion). This mobility, in combination with the fact that a pair of ($J = 1$) molecules has much lower energy when they are nearest neighbors than when they are well separated, causes a significant increase in N_p/N above its value given above for a random distribution and this increase can be observed.[10] The NMR pair spectrum in a single crystal[13] contains a triplet of sharp lines and other structures and depends sensitively on the orientation of the applied magnetic field. In Sec. II A we discuss the nature of the pair spectrum. In solid D_2 the presence of a pair spectrum is only indicated by an absorption line whose width is attributable to pairs, but whose shape is (a) nearly Gaussian and (b) isotropic (i.e., independent of the orientation of the applied magnetic field). The observed weak integrated intensity of this spectrum is consistent with the absence of clustering. Possibly the fact that this spectrum is featureless and isotropic can be explained by assuming that this crystalline field depends on the local environment and therefore varies randomly both in magnitude and in the configuration of its principal axes.

E. Solid echo amplitude

Below we will give a more detailed discussion of the experimental and theoretical situation with regard to the anomalies in the solid echo amplitude: For D_2 (but not for H_2) at ($J = 1$) concentrations below about 0.53 and at temperature below 1 K, when gradual orientational ordering occurs, the solid echo amplitude shows a strikingly anomalous decrease from the expected prediction based on Curie's law. A similar result was obtained in Ref. 8 for the signal from dilute ($J = 1$) H_2 in D_2. We will describe a mechanism that does predict damping of the solid echo amplitude, but which, unfortunately, does not explain the anomalous decrease in the echo amplitude which seems to occur at very short (< 20 μs) echo times. At longer times this theory predicts less dramatic effects from fluctuations which are observed in our experiments. Such an identification does allow us to make an estimate of the amplitude and lifetimes of glasslike fluctuations. Such estimates are otherwise very hard to deduce from experiments.

F. Orientational ordering

In contrast to the above, many properties of these two solids are quite similar. Here we mention only one such property which is relevant to the present paper, namely, the development of long- and short-range orientational order.

In both H_2 and D_2, orientational ordering at zero pressure is due to the same mechanism,[1,9] viz., the electric quadrupole-quadrupole (EQQ) interaction between neighboring molecules with angular momentum $J = 1$ (i.e., o-H_2 or p-D_2). The effective EQQ coupling parameter Γ/k_B is found experimentally[14] to be 0.83 ± 0.04 K for H_2 and 1.04 ± 0.06 K for D_2, some 20% smaller than the theoretical value without renormalizations due to phonons[15,16] or to higher angular momentum states.[14] The transition temperature T_c to the long-range ordered phase for H_2 and D_2 scales approximately with the values of Γ. For the pure ($J = 1$) solids of H_2 and D_2, $T_c = 3.0$ and 4.0 K, respectively, and T_c decreases with decreasing X. The critical value of X at which $T_c(X)$ goes to zero is nearly the same[17,18] for both H_2 and D_2, namely, $X_c = 0.53$. For $X < X_c$ the orientational ordering is short ranged and develops continuously[6] into a glassy state[5] as the temperature is decreased. The orientational fluctuations can be characterized by a correlation time τ_c that increases rapidly from of order 10^{-12} s for $T > 2$ K to about 10^{-8} s when ordering has become substantial at $T \approx 0.4$ K[4,6] and is expected to further increase rapidly as the glassy regime is approached and entered.

G. Outline of this paper

We start by summarizing the experimental situation in Sec. II. In particular, we discuss two NMR phenomena that show striking differences between solid H_2 and D_2. These phenomena both deal with the NMR of species with nuclear spin $I = 1$ (and rotational angular momentum $J = 1$). The first is that the pair spectrum is not observed in D_2 for $X < 0.03$ and the second is that at

intermediate concentrations ($0.2 < X < 0.5$) a dramatic loss of signal amplitude is observed for D_2, in seeming violation of Curie's law. In Sec. III we then present a calculation of the NMR solid echo amplitude which is exact under certain simplifying assumptions and which is useful when the orientational fluctuation time τ_c increases as glasslike orientational freezing takes place. The results of these calculations, where parameters measured or estimated from experiments or predictions are used, are then compared with experiments in Sec. IV. Our conclusions are summarized in Sec. V.

II. THE EXPERIMENTS

A. NMR spectrum of nearest ($J = 1$) neighbor pairs

For o-H_2 impurities in a matrix of solid p-H_2 (with $J = 0$ and $I = 0$), an o-H_2 pair NMR spectrum is observed.[3,13] This experiment led to the first determination of the EQQ coupling parameter Γ. More recently the growth of single crystals has opened up new possibilities and led to the observation of the anisotropy of the NMR spectrum.[13] The analysis gave a determination of the crystalline field splitting V_c of the lowest ($J = 1$) triplet in isolated o-H_2 (Ref. 19) and in the NMR o-H_2 pair spectrum. These values of V_c and Γ were consistent with those determined via microwave absorption.[20] A major reason for the ease in detecting the pair spectrum is its intensity enhancement through the clustering via quantum diffusion. This enhancement becomes ever larger as the temperature is decreased. The single crystal samples that were investigated[13] gave sharp NMR lines with strong anisotropic splittings.

By contrast, the predicted pair spectrum of sharp lines for p-D_2 impurities (with $J = 1$, $I = 1$) in a matrix of solid o-D_2 (with $J = 0$ and $I = 2$ or 0) has not been detected either by cw NMR (Ref. 18) or in solid echo pulse experiments.[4] The latter measurements solely recorded a weak, narrow, approximately Gaussian echo on top of a much larger and much broader echo. A reexamination of these data for $X = 0.05$ shows the ratio of the amplitudes, R, of these two echos to be $R = 0.010 \pm 0.001$. We attribute the strong broad echo signal to ($I = 2$) spins (together with a very small signal due to isolated molecules having $I = 1$) and the weak narrow signal to molecules having $I = 1$ and which exist in clusters of more than one ($J = 1$) molecule.[21] Then the amplitude ratio R should be given by $2X(1 - N_s/N)/[5(1 - X) + 2X(N_s/N)]$, where N_s/N is the fraction of ($J = 1$) molecules which are isolated from other ($J = 1$) molecules. The factors $2X$ and $5(1 - X)$ are the usual nuclear spin amplitudes amplitudes involving $I(I + 1)$ for $I = 1$ and $I = 2$ which occur with relative probabilities X and $(5/6)(1 - X)$. Since $N_s/N = (1 - X)^{12}$, this interpretation would suggest that $R \approx 2X[1 - (1 - X)^{12}]/[5(1 - X)]$, which gives $R = 0.0097$ for $X = 0.05$, in very good agreement with the experimentally deduced value quoted above.

By Fourier transforming the small echo signal from the ($I = 1$) spins which have at least one ($I = 1$) nearest neighbor, the NMR line shape was obtained and the corresponding second moment $M_2(I = 1)$ was calculated and was found to increase smoothly with decreasing T. There was no indication of any structure in the line shape, as was observed in H_2. A careful scan of the echoes at $T = 0.05$ K as the orientation of the applied magnetic field was rotated in 5° steps revealed no evidence of any dependence on the orientation of the magnetic field.[4]

For comparison in Fig. 1(a), we show a representative absorption spectrum of nearest neighbor o-H_2 pairs in a single crystal matrix of p-H_2. This NMR spectrum of ($J = 1$) pairs in solid H_2 is easily understood starting from the expression for the frequency shift $\Delta\nu$ (relative to the Larmor frequency). Initially we ignore intermolecular dipolar interactions, in which case[22]

$$\Delta\nu = \pm(3d/2)\langle 3(\mathbf{J}\cdot\hat{\mathbf{H}})^2 - 2\rangle_J \,, \tag{1}$$

where $\langle\ \rangle_J$ indicates an average over the appropriate rotation quantum states and $\hat{\mathbf{H}}$ is a unit vector in the direction of the applied magnetic field H. Also d is the intramolecular nuclear interaction parameter, whose value, determined from molecular beam experiments,[23] is $d = 57.67$ kHz for H_2 and $d = d_Q + d_M = 25.24$ kHz for D_2. (But these values can have small solid state corrections: For example, see Appendix E of Ref. 22.)

Now we summarize briefly the consequences of Eq. (1). To understand the right-hand side of this equation, we need to refer to the rotational energy level spectrum,[16] reproduced in Fig. 2, for an isolated pair of ($J = 1$)

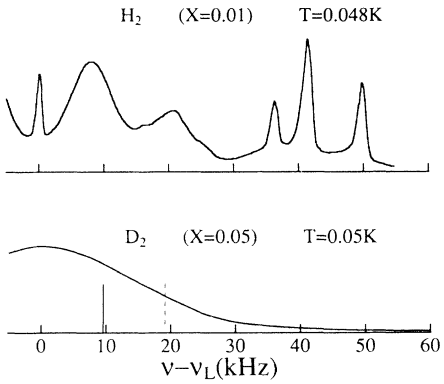

FIG. 1. The ($I = 1$) impurity absorption NMR spectrum for (a) (top) a single crystal of H_2 (Ref. 13). The sharp triplet structure at $\Delta\nu \approx 3d/4 \approx 40$ kHz is due to pairs whose intermolecular axes are parallel to the magnetic field. The broader structure is due to pairs with differently oriented intermolecular axes. (b) (bottom) single crystal spectrum for D_2 with $X = 0.05$ (Ref. 4), where there is no evidence of sharp structures. The vertical solid line corresponds to the center of gravity position of the expected pair signal for a polycrystalline sample. The vertical dashed line indicates the position of the resonance for a pair with intermolecular axis parallel to the magnetic field. [This is the outer limit of the pair spectrum, if the splitting of the lowest doublet of the ($J = 1$) pair levels is neglected. Note that the splitting between components of the triplet, which is due to intermolecular dipolar interactions, is only ~ 0.5 kHz for D_2.]

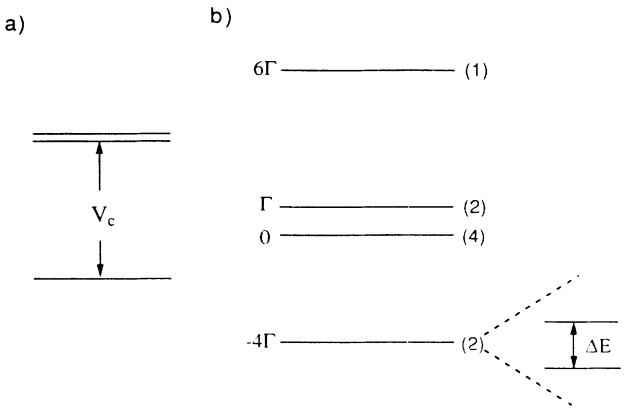

FIG. 2. Energy levels for ($J = 1$) configurations in the otherwise pure ($J = 0$) solid: (a) a single isolated molecule, where the difference between the excited doublet and the ground-state singlet is V_c, (b) an isolated pair of nearest neighbors. The degeneracy of the levels is indicated by parentheses. The energies are in units of the EQQ parameter Γ defined in the text. Due to asymmetric environment of the solid, the lowest doublet of rotational states is split by an energy ΔE as shown on the magnified scale.

molecules in the otherwise pure ($J = 0$) solid. First of all, we assume (as is true for the experimental situations discussed in this paper) that k_BT is small compared to the energy difference between the two lowest rotational energy levels, -4Γ, and the higher excited states. Then we can restrict our attention to these energy levels, which we refer to as the "lowest rotational pair doublet." If the energy splitting ΔE of this doublet is small compared to k_BT, we can take $\Delta E = 0$. For solid H_2 this splitting is known to be of order 0.01 K in temperature units.[20] Then[3]

$$\Delta\nu = \pm(3d/8)(3\cos\theta_{H,\mathbf{n}}^2 - 1) , \qquad (2)$$

where $\theta_{H,\mathbf{n}}$ is the angle between the applied static magnetic field H and $\mathbf{n}$, where $\mathbf{n}$ is a unit vector along the axis joining the two members of the pair. Now the effect of intermolecular dipolar interactions can be included. Interactions with distant ($I = 1$) spins give rise to the usual dipolar broadening. In H_2 for $X \ll 1$, where one can consider the ($I = 1$) spins of the two members of an o-H_2 pair to be nearly isolated from other ($I = 1$) spins, the nuclear dipolar interaction between these two ($I = 1$) spins causes each single resonance given by Eq. (2) to be split into a triplet[3] whose center of gravity is independent of the dipolar interactions, and whose width in energy is of order the nearest neighbor intermolecular dipolar energy. For D_2 this triplet structure may or may not be resolved in the presence of broadening due to ($J = 0, I = 2$) neighbors. But in any event, since the intermolecular dipolar energy is much smaller in D_2 than in H_2, this NMR structure, whether a triplet or a slightly broadened single line, should be observable if solid D_2 were in other respects identical to solid H_2.

Even in a single crystal one does not actually observe a single type of pair. In fact, there are nine different possible axial directions for an o-H_2 pair in a single crystal. Nevertheless, in a hcp single crystal sample, by suitably orienting the sample, one can observe[13] the sharp triplet structure shown in Fig. 1(a) which is the signature of a pair with its axis parallel to the applied field, for which

$$\Delta\nu = \pm(3d/4) . \qquad (3)$$

The other broader structures in Fig. 1(a) are due to pairs with other axial directions. In contrast, when the result of Eq. (2) is averaged over orientations for a powdered sample, each line of the NMR triplet gives rise to a Pake doublet. Then the center of gravity of the resulting triplet feature is at [see Eq. (13) of Ref. 3]

$$\Delta\nu = \pm(3/8)d . \qquad (4)$$

When the lowest rotational pair doublet is split, larger values of $\Delta\nu$ are possible.[24]

Now consider the observed NMR spectrum of D_2. Figure 1(b) shows a representative ($I = 1$) spectrum obtained by processing the solid echo shape observed for $X = 0.05$. Also shown are (a) the expected position for the center of gravity of the triplet one would observe for a powder sample of solid D_2 assuming a sharp pair spectrum as in solid H_2 and (b) the largest splitting one can observe (for molecules whose axis lies along the magnetic field) assuming the rotational pair doublet is unsplit.

Let us discuss the observed NMR spectrum of solid D_2 at low ($J = 1$) concentration.[4] Since no dependence on the orientation of the magnetic field is observed, we assume the sample to be polycrystalline. If the wave functions and energies of the pair states are determined by EQQ interactions alone, we can calculate the NMR pair spectrum as a function of temperature.[3] Using the value $\Gamma/k_B = 1.04$ K for D_2, one calculates that at $T = 1.0$ K practically only the lowest rotational pair doublet manifold is occupied and the second moment is given by $M_2 = (9/80)d^2 \approx 70.\text{kHz}.^2$ (We assume that the splitting of the lowest rotational pair doublet is small compared to k_BT at this temperature. If this assumption is false, M_2 will be even larger.[24]) This calculated value of M_2 is larger than the experimental value of 40 ± 10 kHz (Ref. 4) at 1 K. The fact that at $T = 1$ K the second moment has not yet reached the value predicted for only EQQ interactions indicates that non-EQQ interactions must be present. As T is further decreased, M_2 increases to a value of 90 kHz at 0.1 K and to 170 kHz (Ref. 4) at 0.04 K. This last value would seem to indicate a splitting of the rotational pair doublet $\Delta E/k_B$ is larger than 0.04 K.

We are thus led to speculate that in D_2 the crystalline field is large enough to destroy the sharp NMR triplet spectrum as seen in solid H_2.[25] There, NMR measurements at high pressures[26] showed strong evidence for a substantial increase of the crystalline fields with density, based both on the broadening of the spectrum from single "isolated" molecules [see Fig. 2(a)] and also from the smearing out the pair spectrum. For solid H_2 at a density ρ comparable with that of D_2 at zero pressure, i.e., such that $[\rho(P)/\rho(P = 0) = 1.16]$, we estimate from Fig. 3 of Ref. 26 that the average crystalline field splitting in H_2 is $V_c/k_B = 0.08$ K for "isolated" o-H_2 in p-H_2, while at

$P = 0$,[19,20] $V_c/k_B = 0.008$ K. The analysis of calorimetric data on p-D_2 impurities in o-D_2 (Ref. 27) leads indeed to a crystalline field splitting of order $V_c/k_B \sim 0.1$ K for isolated o-D_2 impurities. However, the analysis has not considered the effects of pairs of ($J = 1$) impurities. Such crystalline fields might modify the "Schottky anomaly" in the specific heat attributed to isolated pairs.[27] But the enhancement of V_c for single impurities in D_2 might suggest similarly larger crystalline fields for pair configurations, and this might be a clue as to why the impurity NMR pair spectra in H_2 and D_2 are so different.

B. NMR ($I = 1$) solid echo amplitude

These experiments are concerned with intermediate concentrations $0.2 < X < 0.5$ of ($J = 1$) molecules, where the orientational ordering can be followed from both static (cw line shapes and solid echo shapes) and from dynamic experiments (longitudinal relaxation time T_1 and stimulated echo decay time τ_E) as a function of temperature. The solid echo amplitude S is proportional to the nuclear spin susceptibility. Because the Larmor frequency $\omega/2\pi = 5.9$ MHz is so much smaller than the thermal frequency $k_BT/h = 10^{12}$ Hz, corresponding to 0.5 K, one expects Curie's law $S \sim T^{-1}$ to be followed.

Indeed for solid H_2, this is found[28] to be true, except at low enough temperatures, where temperature gradients within the sample from ortho–para conversion heating become large. Accordingly, there is a systematic deviation from Curie's law both for cw and for solid echo signals. This deviation is not very different for both detection methods, and diminishes with X, because the heating decreases. Figure 3 shows the extent Curie's law is followed in solid H_2 for $X = 0.50$ and $X = 0.30$, via a plot of the product $A \times T$ versus T. Here A is either the integrated signal in a cw experiment or the solid echo amplitude. If Curie's law were followed, the data points would lie on the horizontal dashed curve.

By contrast, in solid D_2, where the heating rate due to $J = 1$ to $J = 0$ conversion is of order 50 times smaller than in H_2, and hence the temperature inhomogeneities are much less severe, there are strong deviations[4,7] from Curie's law already just below 1 K for the ($I = 1$) echo amplitude signal. However, the ($I = 2$) signal from the o-D_2 molecules follows Curie's law to within about 10%. The observations are the same for the stimulated echo amplitude.[29] These deviations can best be shown by a plot of $S \times T$ versus T, where S is the solid echo (or stimulated echo) amplitude. In Fig. 4, we show such a plot for both the ($I = 2$) and the ($I = 1$) solid echo signals. As can be seen, the product $S \times T$ for the ($I = 1$) signal has a minimum for $X = 0.45$. Combining the results for solid echo[7] and stimulated echoes,[29] for X between 0.4 and 0.55, it is found that the temperature of this minimum decreases with X and extrapolates to zero for $X \approx 0.33$, as seen in Fig. 5. Even at lower X, where a minimum in $S \times T$ was not observed, the deviation from Curie's law is still significant, as can be seen in Fig. 4.

A note of explanation about the solid echo technique is necessary here: The echo signal is formed with a peak at a time τ after the second rf pulse of a two-pulse sequence spaced by τ. The sequence is written as $\beta_1 - \tau - \beta_{2,\phi}$, where β_1 and β_2 are the pulse tipping angles, usually with $\beta_1 = 90°$, and ϕ is the phase angle of the second pulse with respect to the first one. The sequences are labeled xx for $\phi = 0$ and xy for $\phi = 90°$, and the echo amplitudes $S(2\tau)$ are functions of τ and of various parameters appearing in the spin Hamiltonian. Theory[30] for the solid echo of spins $I = 1$ shows that the sum of

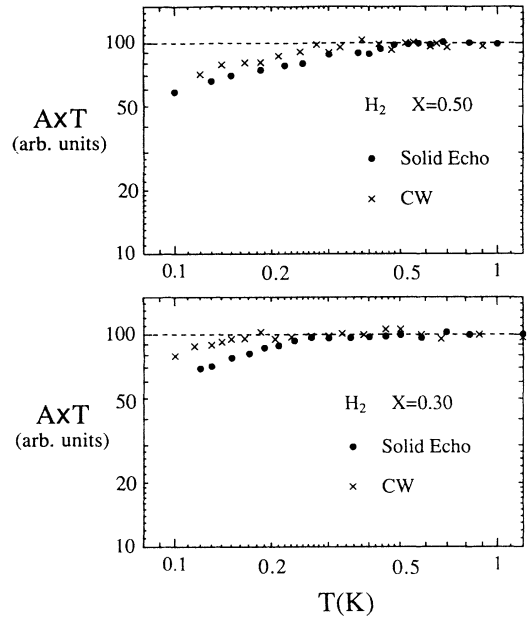

FIG. 3. The product $A \times T$ vs T, normalized to 100 at 1.0 K for solid H_2, where A is either the integrated NMR absorption line (crosses) from cw experiments or the solid echo amplitude (solid circles) (from Fig. 2 of Ref. 28). Top: $X = 0.50$. Bottom: $X = 0.30$.

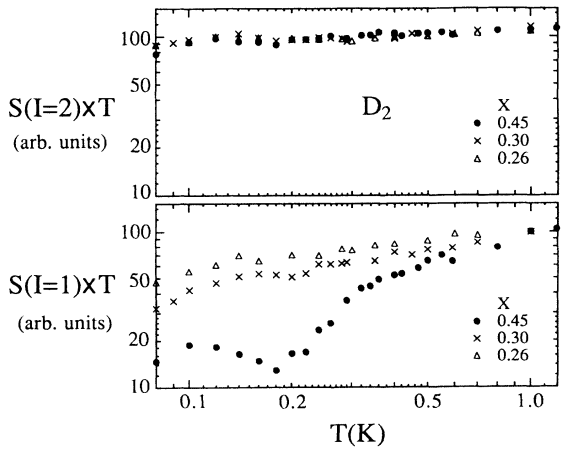

FIG. 4. The product $S \times T$ vs T, normalized to 100 at 1.0 K for solid D_2 for the ($I = 1$) and the ($I = 2$) spin systems at various concentrations $X(J = 1)$, where S is the solid echo amplitude (from Ref. 7).

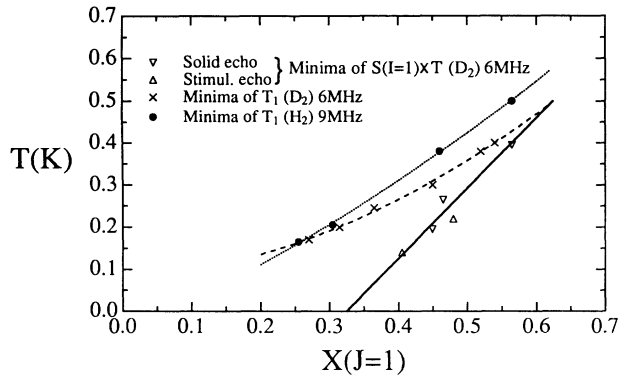

FIG. 5. The location of the minima in $S \times T$ for D_2 ($I = 1$) signal (triangles) (from Ref. 29), and location of the minima in the longitudinal relaxation times in D_2 at 6 MHz (Ref. 4) and in H_2 at 9 MHz (Ref. 28). The fitted curves are merely guides to the eye.

absolute values,

$$S_{\rm tot}(2\tau) = |S_{xy}(2\tau)| + |S_{xx}(2\tau)| \,, \qquad (5)$$

is a function of the intermolecular dipolar interaction fields alone, where contributions to the damping from other sources are canceled out. (This result is rederived below.) Plots of $S_{\rm tot}$ versus τ for solid H_2 (Ref. 30) and D_2 (Ref. 7) lead to a determination of the intermolecular dipolar parameters, and at first glance, these appear to be temperature independent within the scatter. The echo amplitudes $S_{\rm tot}$ shown in Fig. 4 are extrapolated to $\tau = 0$ from the experimental range 30 μs $< \tau < 1.2 \times 10^3$ μs over which $S_{\rm tot}$ decays by a factor of about 40. (See Fig. 2 of Ref. 7.) Hence they are assumed to represent the echo amplitude free of any decay.

In Fig. 5 we have shown the location of $T_{\rm min}(X)$, the temperature of the minimum of the $S \times T$ product. It is interesting to compare $T_{\rm min}(X)$ with the temperature $T_{T_1,{\rm min}}(X)$, where the longitudinal relaxation time is a minimum. This latter temperature occurs approximately when $\omega_L \tau_c = 0.6$,[4] namely, where $\tau_c = 1.6 \times 10^{-8}$ s for $\omega_L/2\pi = 5.9$ MHz. The dependence of $T_{T_1,{\rm min}}(X)$ on X is roughly similar to that of $T_{\rm min}(X)$. One might therefore be tempted to search for a relationship between the observed "spin loss" and the fluctuation correlation time τ_c. However, in Fig. 5 we also show by the dashed curve the line $T_{T_1,{\rm min}}(X)$ for H_2 for the experiments done with $\omega_L = 2\pi \times 9$ MHz., i.e., corresponding to a minimum T_1 for $\tau_c = 1.1 \times 10^{-8}$ s. This line has a similar trend as that for D_2, but the solid echo amplitude behavior in H_2 does not show a comparable spin loss.

The obvious question, whether such an anomalous behavior can be detected by cw methods, cannot readily be answered because of the difficulties in trying to observe with sufficient accuracy the weak and broad ($I = 1$) signal in D_2. A cw study that uses the very sensitive liquid-helium-cooled NMR spectrometer developed by Hardy and Gray[31] for measurements in the ordered phase[32] with $X \approx 1$, applied to lower X, would be very interesting indeed.

Solid echo experiments for D_2 indicate an effective ($I = 1$) spin loss as orientational ordering proceeds in the hcp phase. No such loss has been observed[33] in the long-range ordered phase, except possibly near the transition (see Fig. 2 of Ref. 33 and discussion in the text). To what can the spin loss in the short-range ordering regime, above and within the glasslike phase be attributed? Here are some possible, but not very likely scenarios.

(1) Possibly due to some anomalous and unexplained inhomogeneous broadening, a fraction of the spins could give rise to a very broad, say, more than 100 kHz wide, NMR line. Such a broad signal cannot be observed by the solid echo techniques.[7] cw techniques would also be unable to detect this weak broad signal.

(2) There might be a rapid decay of the echo amplitude envelope at times so short ($\tau < 10$ μs) that it cannot be observed. This scenario would require anomalous damping of the echo due to large time-fluctuating fields. The slower decay of the echo envelope which we observe at longer times (i.e., for $\tau > 50$ μs) is mainly due to intermolecular dipolar interactions. This decay is, however, also affected by the orientational fluctuation rates τ_c^{-1} which decrease strongly as T is decreased below 1 K, as will be discussed in detail in Sec. III.

(3) In D_2 the intramolecular parameter d results mostly from the nuclear quadrupolar interaction term $d_Q = 23$ kHz while the dipolar contribution is relatively small, $d_M = 2$ kHz. By contrast, in H_2, $d_Q = 0$ and $d_M = 57$ kHz. Perhaps the nuclear spin Hamiltonian for ($I = 1$), ($J = 1$) in D_2 is really different from the ($J = 1$), ($I = 1$) Hamiltonian in H_2.

(4) A final possibility is that, in contrast to (1), a fraction of the ($I = 1$) spins unexpectedly becomes located in a sharper line centered at the Larmor frequency and having a width comparable to that of the ($I = 2$) spins. This would imply that these "missing" ($I = 1$) spins have an anomalously small short-range ordering, comparable with that of the ($I = 2$) spins. The NMR lines from the two different spin species could then not be resolved, and they would both contribute to the amplitude of the broad spin echo.

None of these explanations is satisfactory, as we now discuss. For instance, mechanism (1) has been invoked[34] to explain the analogous loss of signal in spin glasses. There, however, it is plausible to posit the existence of large inhomogeneous broadening due to randomly placed paramagnetic impurities. In D_2 there is no justification to use such an explanation. Mechanism (2) is analyzed in detail in the next section, where we find that although it gives rise to some small effects, it cannot explain the very large loss in signal amplitude seen in experiment. Mechanism (3) seems to be excluded by the fact that the large loss of signal was also seen[8] when dilute ($J = 1$) H_2 was used to probe the glassy orientational state of D_2. Finally, if the scenario proposed as mechanism (4) actually occurred, the amplitude of the broad echo [from all the ($I = 2$) plus a fraction of ($I = 1$) spins] would then become larger than predicted from Curie's law. In Fig. 4, the product $S(I = 2) \times T$ would then pass over a maximum when $S(I = 1) \times T$ passes through a minimum. For $X = 0.46$ one calculates that $S(I = 2) \times T$ should peak at 125 (in the units of Fig. 4) for $T = 0.18$ K. This

is contrary to observation and therefore this possibility is excluded.

III. EFFECT OF FLUCTUATIONS ON THE SOLID ECHO AMPLITUDE

In this section we present a theory for the amplitude decay of the solid echo as a function of the pulse spacing time τ which includes the effects of fluctuations in the quadrupole field tending to orient the molecules. Heretofore, calculations have treated the case where each molecule is in a static crystalline field. While this approximation is often a sufficient one to model the effect of EQQ interactions, it will fail if the time scale for fluctuations in the EQQ interaction becomes comparable to the time scale on which the solid echo is observed. This calculation is the clearest in a simplified model in which intermolecular dipolar interactions are ignored and this case is considered first. Later we discuss a qualitative way to include intermolecular interactions. The application of this theory to experimental data is then discussed.

We consider N noninteracting nuclear spins (of magnitude 1) $\mathbf{I}_j$, whose Hamiltonian is $\mathcal{H} = \hbar \sum_j h_j$, where

$$h_j = \alpha_j I_{j,z} + \gamma_j I_{j,z}^2 \,. \tag{6}$$

Here α_j is the Larmor frequency of the jth spin and γ_j represents the effect of the nuclear quadrupolar splitting of the jth nuclear spin. In the present context this splitting is time dependent since it actually depends on the orientation of the jth molecule, which in turn is determined by the EQQ interactions with its neighboring molecules. We write γ_j as the sum of a time-independent static component and a time-fluctuating part:

$$\begin{aligned}\gamma_j &= \frac{15d}{2}\left[\frac{1}{2} - \frac{3}{2}\cos^2\theta_j(t)\right] \\ &= \frac{3d}{2}\left[3J_{z,j}(t)^2 - 2\right] \\ &\equiv \langle\gamma_j\rangle + [\gamma_j(t) - \langle\gamma_j\rangle] \,,\end{aligned} \tag{7}$$

where θ_j is the angle between the jth molecular axis and the applied field H and $\langle\ \rangle$ indicates a time-averaged value. The magnitude of the fluctuating term is characterized by its root mean square value,

$$\tilde{\gamma}_j \equiv \langle(\gamma_j(t) - \langle\gamma_j\rangle)^2\rangle^{1/2} = \left[\langle\gamma_j^2\rangle - \langle\gamma_j\rangle^2\right]^{1/2} \,. \tag{8}$$

To calculate the echo amplitude we start from the expression for the NMR signal after the spins are subject to rf pulses at times 0 and τ with associated pulse angles $\beta_1 = 90°$ and β_2, respectively, and are then observed at time t, where we will be interested in the case $t = 2\tau$. The signal $S_+(t)$ at time t is given by[30]

$$S_+(t) = \sum_{j,k} \frac{1}{2N3^{N-1}} \mathrm{Tr}\left[R^+ e^{-i(h_j+h_k)\tau} I_{j,x} e^{i(h_j+h_k)\tau} R e^{i(h_j+h_k)(t-\tau)} I_{k,+} e^{-i(h_j+h_k)(t-\tau)}\right] \,. \tag{9}$$

Here Tr indicates a trace over all 3^N spin states, $R = \prod_j r_j$, where r_j is the rotation matrix for the jth spin, which is given by Yu *et al.*[30] (Eq. B5) as

$$r_j = c + \frac{1}{2}(1+c)I_{jz}^2 + \frac{1}{2}s(e^{-i\phi}I_{j+} - e^{i\phi}I_{j-}) + \frac{1}{4}(1-c)(e^{-2i\phi}I_{j+}^2 + e^{2i\phi}I_{j-}^2) \,, \tag{10}$$

where $c \equiv \cos\beta_2$ and $s \equiv \sin\beta_2$ and ϕ characterizes the phase of the second pulse relative to the first one.

First we consider the case when $\tilde{\gamma}_j = 0$, i.e., when there are no fluctuations.[30] We substitute $R = \prod_l r_k$ into Eq. (9). In the resulting product, terms with $l \neq j$ and $l \neq k$ can be simplified using $r_l^+ r_l = I$, the unit operator. So

$$\begin{aligned}S_+(t) = &\sum_{j,k}{}' \frac{1}{2N3^{N-1}} \mathrm{Tr}\left[r_j^+ r_k^+ e^{-i(h_j+h_k)\tau} I_{j,x} e^{i(h_j+h_k)\tau} r_k r_j e^{i(h_j+h_k)(t-\tau)} I_{k,+} e^{-i(h_j+h_k)(t-\tau)}\right] \\ &+ \sum_j \frac{1}{2N3^{N-1}} \mathrm{Tr}\left[r_j^+ e^{-ih_j\tau} I_{j,x} e^{ih_j\tau} r_j e^{ih_j(t-\tau)} I_{j,+} e^{-ih_j(t-\tau)}\right] \,,\end{aligned} \tag{11}$$

where the prime indicates the term $j = k$ is to be excluded. Now trace over all states of spins l with l not equal to j or to k. In so doing note that the terms with $j \neq k$ vanish. So

$$S_+(t) = \frac{1}{2N} \sum_j \mathrm{tr}\left[r^+ e^{-ih\tau} I_x e^{ih\tau} r e^{ih(t-\tau)} I_+ e^{-ih(t-\tau)}\right] \,, \tag{12}$$

where, for notational simplicity, we omit the subscripts j so that $r \equiv r_j$, $I_x \equiv I_{x,j}$, etc., and tr will mean a trace over spin states of the jth spin. Explicitly, we have

$$S_+(2\tau)=\frac{1}{2N}\sum_{m,j}\Big[\langle 0|r^+|m\rangle\langle m|e^{-ih\tau}|m\rangle\langle m-1|e^{ih\tau}|m-1\rangle\langle m-1|r|1\rangle\langle 1|e^{ih\tau}|1\rangle$$
$$+\langle 0|r^+|m\rangle\langle m|e^{-ih\tau}|m\rangle\langle m+1|e^{ih\tau}|m+1\rangle\langle m+1|r|1\rangle\langle 1|e^{ih\tau}|1\rangle$$
$$+\langle -1|r^+|m\rangle\langle m|e^{-ih\tau}|m\rangle\langle m-1|e^{ih\tau}|m-1\rangle\langle m-1|r|0\rangle\langle -1|e^{-ih\tau}|-1\rangle$$
$$+\langle -1|r^+|m\rangle\langle m|e^{-ih\tau}|m\rangle\langle m+1|e^{ih\tau}|m+1\rangle\langle m+1|r|0\rangle\langle -1|e^{-ih\tau}|-1\rangle\Big]\,. \tag{13}$$

Here we used the fact that $\langle 0|e^{ih\tau}|0\rangle=1$. Then

$$S_+(2\tau)=\frac{1}{4N}\sum_j\Big[c(1-c)e^{i\tau(-\alpha_j+\gamma_j)}e^{2i\phi}e^{i\tau(\alpha_j+\gamma_j)}-s^2e^{i\phi}e^{-i\tau(\alpha_j+\gamma_j)}e^{i\phi}e^{i\tau(\alpha_j+\gamma_j)}$$
$$+c(1+c)e^{i\tau(\alpha_j+\gamma_j)}e^{2i\phi}e^{i\tau(\alpha_j+\gamma_j)}+s^2e^{-i\phi}e^{-i\tau(-\alpha_j+\gamma_j)}e^{i\phi}e^{i\tau(\alpha_j+\gamma_j)}$$
$$+c(1-c)e^{2i\phi}e^{-i\tau(\alpha_j+\gamma_j)}e^{-i\tau(-\alpha_j+\gamma_j)}-s^2e^{i\phi}e^{i\tau(-\alpha_j+\gamma_j)}e^{i\phi}e^{-i\tau(-\alpha_j+\gamma_j)}$$
$$+c(1+c)e^{-i\tau(-\alpha_j+\gamma_j)}e^{-i\tau(-\alpha_j+\gamma_j)}+s^2e^{i\phi}e^{i\tau(\alpha_j+\gamma_j)}e^{-i\phi}e^{-i\tau(-\alpha_j+\gamma_j)}\Big]\,, \tag{14}$$

$$S_+(2\tau)\equiv Ae^{2i\phi}+\frac{1}{N}\sum_j B_je^{2i\tau\alpha_j}\,, \tag{15}$$

where

$$A=\frac{1}{2N}\sum_j\Big[c(1-c)\cos(2\tau\gamma_j)-s^2\Big]\,, \tag{16}$$

$$B_j=\frac{1}{2}\Big[c(1+c)\cos(2\tau\gamma_j)+s^2\Big]\,. \tag{17}$$

We can now generalize to time-dependent γ_j. To do this, note that in Eq. (13) the rightmost factors of $\exp(ih\tau)$ come from the time interval between times τ and 2τ, whereas the leftmost such factors come from the time interval between 0 and τ. So we have

$$S_+(2\tau)=\frac{1}{2}e^{2i\phi}\Big[-s^2\Big\langle\cos\Big(\int_0^\tau\gamma_j(t)dt-\int_\tau^{2\tau}\gamma_j(t)dt\Big)\Big\rangle_j$$
$$+c(1-c)\Big\langle\cos\Big(\int_0^{2\tau}\gamma_j(t)dt\Big)\Big\rangle_j\Big]$$
$$+\frac{1}{2}s^2\Big\langle e^{2i\tau\alpha_j}\cos\Big(\int_0^\tau\gamma_j(t)dt-\int_\tau^{2\tau}\gamma_j(t)dt\Big)\Big\rangle_j$$
$$+\frac{1}{2}c(1+c)\Big\langle e^{2i\tau\alpha_j}\cos\Big(\int_0^{2\tau}\gamma_j(t)dt\Big)\Big\rangle_j\,. \tag{18}$$

Now we drop the rapidly fluctuating intramolecular dipolar interactions. Within this approximation we no longer have the correct behavior in the limit $\tau\to 0$. But for times such that $\tau d>>1$ we have

$$S_+(2\tau)=-\frac{s^2}{2}e^{2i\phi}\Big\langle\cos\Big(\int_0^\tau\gamma_j(t)dt-\int_\tau^{2\tau}\gamma_j(t)dt\Big)\Big\rangle_j+\frac{s^2}{2}\Big\langle e^{2i\tau\alpha_j}\cos\Big(\int_0^\tau\gamma_j(t)dt-\int_\tau^{2\tau}\gamma_j(t)dt\Big)\Big\rangle_j\,. \tag{19}$$

Note that the fluctuations in γ_j are incorporated in the factor

$$Z_j\equiv\exp\Big(i\int_0^\tau\gamma_j(t)dt-i\int_\tau^{2\tau}\gamma_j(t)dt\Big)\,. \tag{20}$$

Note that Z_j does not depend on $\langle\gamma_j\rangle$. Thus, if $\gamma_j(t)$ is constant in time, $\langle Z_j\rangle_j=1$ and there is no fluctuation effect. Now, including fluctuations, we have

$$S_j(2\tau)=-\frac{1}{2}s^2e^{2i\phi}\mathrm{Re}\langle Z_j\rangle_j+\frac{1}{2}s^2\langle e^{2i\alpha_j\tau}\mathrm{Re}Z_j\rangle_j\,, \tag{21}$$

which we assume is the same as

$$S_j(2\tau)=-\frac{1}{2}s^2e^{2i\phi}\mathrm{Re}\langle Z_j\rangle_j+\frac{1}{2}s^2\langle e^{2i\alpha_j\tau}\rangle_j\mathrm{Re}\langle Z_j\rangle_j\,. \tag{22}$$

So we will now analyze the crucial quantity $\langle Z_j\rangle_j$. There are actually two averages here: one over time, the other over configurations. We will assume that these averages are not correlated. We will simply interpret $\langle\ \rangle_j$ to be an average over the distribution of the stochastic variable $\gamma_j(t)$, whose distribution is assumed to be independent of j. Define

$$\sigma(t) = +1\ , \quad 0 < t < \tau$$
$$= -1\ , \quad \tau < t < 2\tau\ , \tag{23}$$

so that

$$\langle Z_j \rangle_j = \left\langle \exp\left(i \int_0^{2\tau} \gamma_j(t)\sigma(t)dt \right) \right\rangle_j . \tag{24}$$

Now we assume temporal correlations of the form

$$\langle \gamma_j(t)\gamma_j(t+\tau)\rangle_j - \langle \gamma_j(t)\rangle^2 = \tilde{\gamma}^2 F(|\tau/\tau_c|)\ , \tag{25}$$

where we require $F(0) = 1$, so that $\tilde{\gamma}$ is the rms amplitude of the random fluctuations, as in Eq. (8), and we have indicated that the time correlation function is expected to be a function of time scaled by the orientational correlation time τ_c. In fact, we assume the fluctuations are Gaussian, with the above correlation matrix, as implied by Eq. (25). That being the case, we have

$$\langle Z_j \rangle_j = \exp\left[-\frac{1}{2}\tilde{\gamma}^2 \int_0^{2\tau} ds\sigma(s) \int_0^{2\tau} dt\sigma(t) F(|s-t|/\tau_c|) \right]. \tag{26}$$

This is our principal result and it is clearly of the form to be expected. To see the consequences of the above result, let us use a simple special form for $F(x)$, namely, $F(x) = e^{-x}$. Then we find

$$\langle Z_j \rangle_j = \exp\{-\tilde{\gamma}^2(2\tau\tau_c - \tau_c^2[3 - 4e^{-\tau/\tau_c} + e^{-2\tau/\tau_c}])\}\ . \tag{27}$$

There are obviously two limiting cases of this. First, when $\tau_c \ll \tau$ (the usual case), we have

$$\langle Z_j \rangle_j = \exp(-2\tilde{\gamma}^2\tau\tau_c)\ . \tag{28}$$

In the other limit, i.e., when $\tau_c \gg \tau$, then

$$\langle Z_j \rangle_j = \exp[-(2/3)\tilde{\gamma}^2\tau^3/\tau_c]\ . \tag{29}$$

In the former limit, one just has a small addition onto the intermolecular relaxation rate. In the latter limit, there are two subcases. If $\tau_c \gg \tau$ so that Eq. (29) applies, and in fact is so large that $\tilde{\gamma}^2\tau^3/\tau_c$ is small, then fluctuations have almost no effect. However, in a crossover regime when $\tau_c \gg \tau$ so that Eq. (29) applies, but τ_c is still small enough that $\tilde{\gamma}^2\tau^3/\tau_c$ is large (this can happen if $\tilde{\gamma}\tau$ is large), then one loses signal. To be explicit, this crossover regime is defined by

$$1 \ll \tau_c/\tau \ll (\tilde{\gamma}\tau)^2\ . \tag{30}$$

Since the first term in Eq. (22) is larger in magnitude than the second, the amplitude $S_{\rm tot} = |S_{xx}| + |S_{xy}|$ is given by

$$S_{\rm tot}^F = s^2 {\rm Re}\langle Z_i \rangle_i \equiv s^2 Z^F(\tau, \tau_c)\ , \tag{31}$$

where now the damping contribution $\langle e^{2i\alpha_i\tau}\rangle_i$ has been eliminated. Here the superscript F indicates that we only include the effects of temporal fluctuations. The larger effect of intermolecular dipolar interactions is not yet included. A simpleminded way to include them is to set

$$S_{\rm tot} = s^2 Z^F Z^{\rm dip}\ , \tag{32}$$

where $s^2 Z_i^{\rm dip}$ is given by Eq. (22) in Ref. 30 and is only a function of intermolecular dipolar interaction, and therefore temperature independent. An observed temperature dependence in $S_{\rm tot}$ is the unique signature of Z^F.

Now we consider the case when the correlations have a different type of time dependence. For instance, in models of orientational glasses it has been found[35] that these correlations are described by a stretched exponential, i.e.,

$$F(x) = \exp(-|x|^y)\ , \tag{33}$$

where y is the exponent for stretching the exponential. Computer simulations[35] show that for the model of an isotropic orientational glass, y varies from 1 in the high-temperature regime, where the system is orientationally disordered and the correlation time τ is very short (say, 10^{-12} s) to 0.7 at a characteristic spin glass temperature, and finally to 0.3 at temperatures well inside the glassy state. For the situation with $y < 1$ we must evaluate Z^F numerically.

We first deal with results for $y = 1$, the simple exponential decay. Here we have chosen the range 50 μs $< \tau < 1.2 \times 10^3$ μs which corresponds to the experimental conditions for D_2. Over this range, as mentioned before, the measured echo amplitude $S_{\rm tot}$ decays by a factor of about 40, and we interpret the decay as to be mostly due to intermolecular dipolar interaction, which is temperature independent. The additional (temperature dependent) decay from the orientational fluctuations alone must therefore be comparatively small. The calculated Z^F from Eq. (27) only reflects the latter decay and is shown in Fig. 6 as a three-dimensional plot versus τ and τ_c for D_2. Here we have chosen a representative range for τ_c, namely, between 10^{-8} and 1 s, which for both D_2 and H_2 at $X = 0.55$ would apply to temperatures below approximately 0.8 K. The larger values of

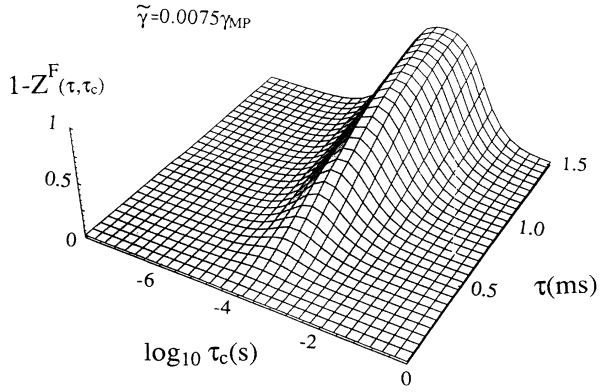

FIG. 6. Three-dimensional plot of the calculated $Z(\tau, \tau_c) \equiv Z^F$ for D_2 for an exponential decay of the correlation function, as per Eq. (27), for $\tilde{\gamma} = 0.0075\tilde{\gamma}_{\rm MP}$.

τ_c correspond to progressively lower temperatures where the sample might be in a glassy state. For application to D_2 we have used as a first guess $\tilde{\gamma} = 0.0075\gamma_{MP}$, where $\gamma_{MP} = (2\pi)3d/2 = 2.4 \times 10^5$ rad/s is the most probable static value,[30] i.e., when the applied field is perpendicular to the molecular axis. As can be seen, the decay of Z^F is negligible for $\tau_c < 10^{-6}$ s, but increases as τ_c increases, and this decay is maximized when $\tau_c = \tau/2$, as shown in Fig. 7(a) in a plot of Z^F versus τ_c for given values of τ. Also we note from Eq. (27) that the damping strongly increases with $\tilde{\gamma}$. Since Z is a strong function of τ_c, this implies that it should be temperature dependent. Finally, in Fig. 7(b) we give a similar plot for parameters appropriate for H_2, where we use $d = 57.67$ kHz,[23] which approximately doubles the value of $\tilde{\gamma}$. But more significantly, the experimental range of τ, which in practice is determined by the decay due to intermolecular interactions, is an order of magnitude smaller for H_2 than for D_2. From Fig. 7(b) we conclude that fluctuation effects in Z are much smaller in H_2 than in D_2.

IV. DISCUSSION OF EXPERIMENTAL RESULTS

The observed decay of S_{tot} for the $(I = 1)$ spins in D_2 is shown in Fig. 8 for three concentrations at various temperatures, where the amplitude at $\tau = 0$ has been normalized in each part. It can be seen that the decay at the highest concentration $X = 0.46$ is largest at $T = 0.2$ K, which is the temperature of the largest deviation of the solid echo amplitude from Curie's law (Fig. 4). (We observed a similar temperature dependence of the decay, not shown here, for $X = 0.48$.) The difference between the decays at various temperatures is found to be smaller at $X = 0.30$ (where the decay is largest at $T = 0.1$ K) and disappears for $X = 0.22$, where the signal-to-noise ratio has become poor for large τ. In Fig. 9 we show the decay of S_{tot} for the $(I = 2)$ spins for $X = 0.46$ for the same temperatures as in Fig. 8. Within the exper-

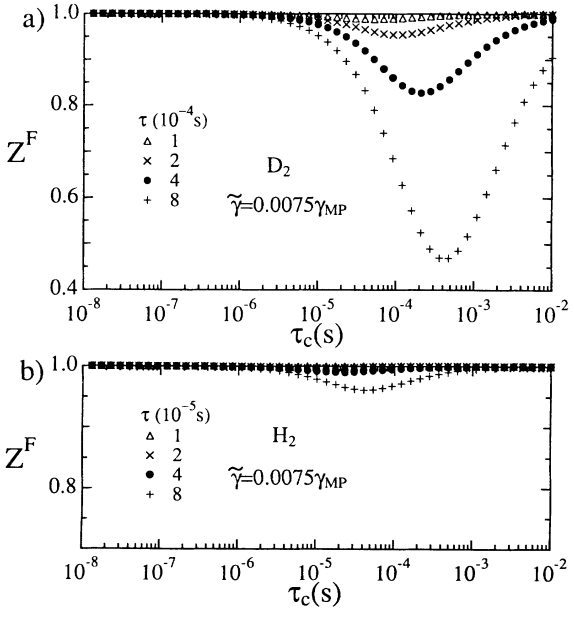

FIG. 7. Plot of $Z^F(\tau, \tau_c)$ vs τ_c for given values of τ and for $\tilde{\gamma} = 0.0075\tilde{\gamma}_{MP}$ with $\tilde{\gamma}_{MP} = 3d/2$: (a) for D_2 for the experimental range of τ, (b) for H_2 for the experimental range of τ.

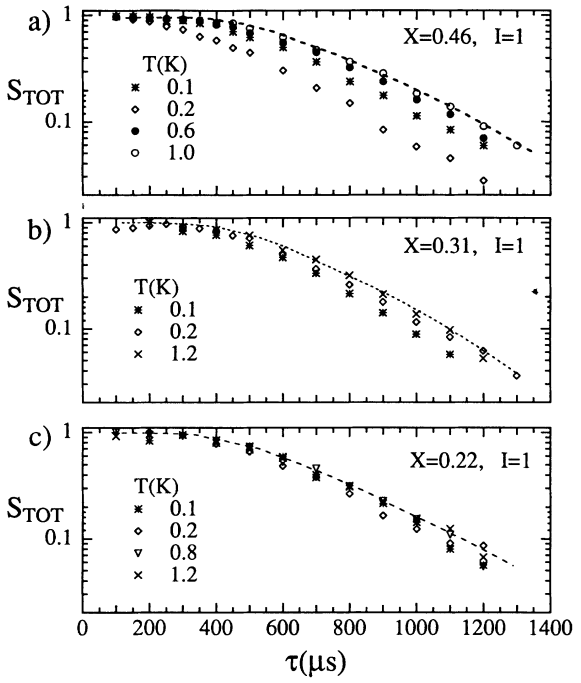

FIG. 8. The observed decay of S_{tot} for $(I = 1)$ spins vs τ at various temperatures for (a) $X = 0.45$, (b) $X = 0.31$, and (c) $X = 0.22$.

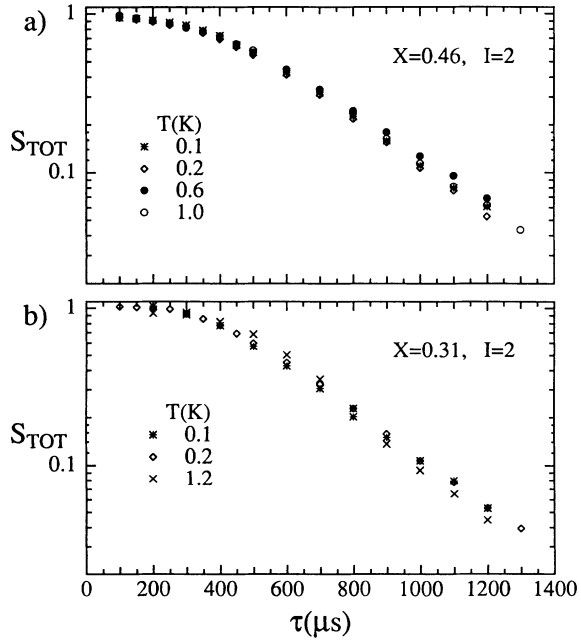

FIG. 9. The observed decay of S_{tot} for $(I = 2)$ spins vs τ at various temperatures: (a) $X = 0.46$ and (b) $X = 0.31$.

imental uncertainty there is no trend of a temperature dependence in the decay. The degree of orientational ordering of o-D_2 molecules with $I = 2$, as shown by the order parameter (see Figs. 7 and 10 in Ref. 4), is much smaller than for the p-D_2 molecules, and hence for them $\tilde{\gamma}$ (which is proportional to the order parameter) is drastically reduced. Thus even though τ and τ_c are the same for the $(I = 2)$ spins as for the $(I = 1)$ ones, Eq. (27) shows that $Z^F \approx 1$ and no fluctuation effect is expected for the $(I = 2)$ signal, in agreement with experiment.

Returning to the experimental results in Fig. 8(a), we now consider the decay of $S_{\rm tot}$ at $T = 0.6$ and 1.0 K to be entirely caused by intermolecular dipolar interactions, and represented by $Z^{\rm dip}$. The values of $Z^{\rm dip}$ have been discussed in Ref. 7, where they are shown to be consistent with the known intermolecular dipolar interactions. Using these values of $Z^{\rm dip}$ and the experimentally observed values of $S_{\rm tot}$ in Eq. (32), we obtain Z^F for various temperatures, as presented in Fig. 10, where for clarity we only show the isotherms 1.0, 0.2, and 0.1 K for $X = 0.46$. Furthermore, in Fig. 11 we recast the plot as a function of T for various values of τ. To each value of T corresponds a given value τ_c. From the discussion above, the maximum damping at $T = 0.2$ K occurs for $\tau = 2\tau_c$ and hence this indicates that τ_c is approximately 400 μs. Now we try to fit the experimentally determined curves of Z^F versus τ with a suitable choice of τ_c and $\tilde{\gamma}$. Such fits are shown in Fig. 10 for $T = 0.2$ K and $T = 0.1$ K by solid and dashed lines, respectively. We find $\tilde{\gamma} = 0.007\gamma_{\rm MP}$ and $\tau_c = 450$ μs for $T = 0.2$ K and $\tilde{\gamma} = 0.007\gamma_{\rm MP}$ and $\tau_c = 4.0$ ms for $T = 0.1$ K.

As can be seen, the fit of theory to experiment is only fair, and there are systematic differences: In particular at small times τ, experimental data indicate a larger damping than given by theory. Because a two-parameter ($\tilde{\gamma}$ and τ_c) fit was used, there is a correlation between them to obtain the "best fit." The error bars in Fig. 12 indicate the uncertainties due to this correlation. For instance, at $T = 0.2$ K, an approximately equally good fit is obtained in Fig. 10 for $\tau_c = 600$ μs and $\tilde{\gamma} = 0.004\gamma_{\rm MP}$. However, because of the various assumptions made to enable

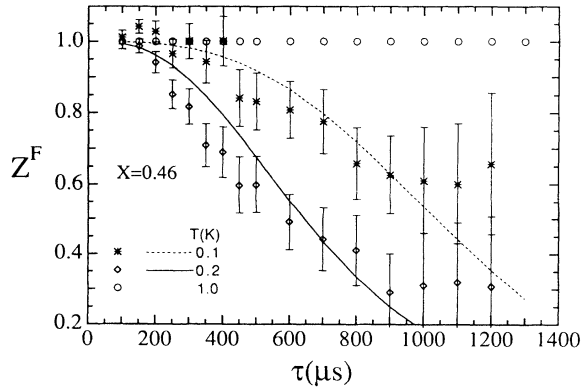

FIG. 10. Plot of Z^F vs τ, obtained from data for $X = 0.46$ via Eq. (32), and for $T = 1.0$, 0.2, and 0.1 K. The solid and dashed lines are the fit of Eq. (27) to the data with $\tilde{\gamma} = 0.0075\gamma_{\rm MP}$ and $\tau_c = 450$ μs for $T = 0.2$ K and $\tilde{\gamma} = 0.007\gamma_{\rm MP}$ and $\tau_c = 4.0$ ms for $T = 0.1$ K.

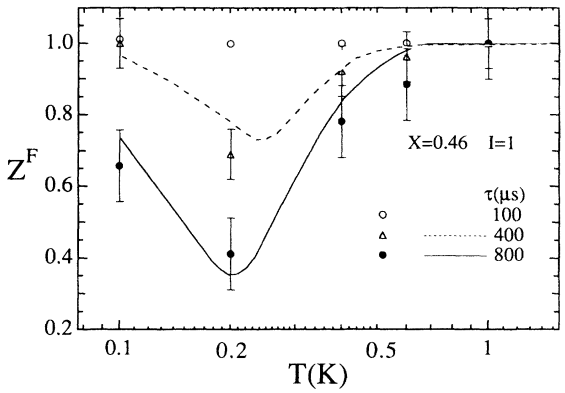

FIG. 11. Z^F vs T for various values of τ. The points are the experimentally deduced values of Z^F with associated uncertainties represented by error bars. The solid and the dashed lines are the calculated curves when $\tilde{\gamma}_0$ and τ_c are given by the curves in Fig. 12.

the data analysis to be tractable — such as assuming the stretch exponent y to be unity — we have to limit our error discussion. Our results as shown in Fig. 12 therefore have a large uncertainty.

The next step consists in checking how consistent the τ_c at 0.2 K is with that from determinations of τ_c^* from longitudinal relaxation measurements. Here we use (1) the high-temperature approximation, Eq. 5 of Ref. 4, where τ_c^* is determined from the relaxation time of the $(I = 1)$ spin system, τ_s. (2) the relation $\omega\tau_c^* = 0.6$ (Eq. 3 of Ref. 4) at the minimum of τ_s, which for $\omega/2\pi = 5.9$ MHz gives $\tau_c^* = 1.6 \times 10^{-8}$ s, as mentioned in connection with our Fig. 5. These points for $X = 0.46$

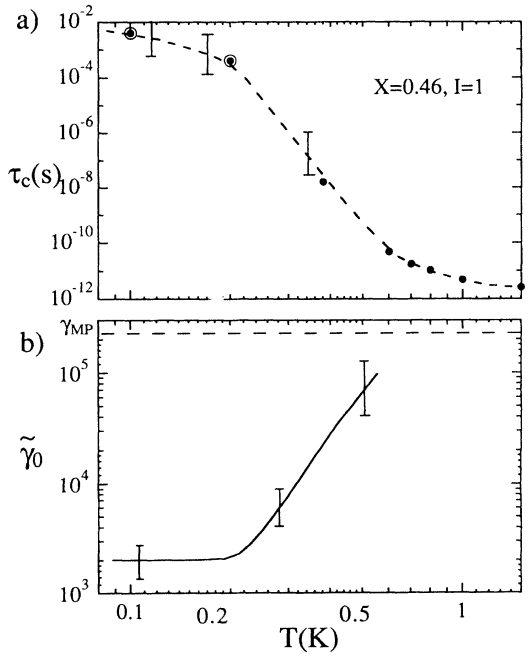

FIG. 12. (a) The correlation times τ_c from NMR measurements at $X = 0.46$. Solid circles: τ_c^* from longitudinal relaxation times (Ref. 4). Concentric circles: from a fit of the calculated Z^F to the data. Dashed curve: $\tau_c(T)$ giving a reasonable representation of the data in Figs. 9 and 10, in combination with $\tilde{\gamma}(T)$, shown in panel (b).

are shown in Fig. 12(a) by solid circles, while the present determination smoothly extends the data. In order to achieve agreement with the experimental data for Z^F at all temperatures, $\tilde{\gamma}$ has to increase with T; otherwise, the calculated Z^F decreases much faster with increasing T than shown by experiment (solid circles and triangles in Fig. 11). Of course, $\tilde{\gamma}$ cannot become larger than γ_{MP}. Combining the curves for the best estimate of τ_c (dotted line) and of $\tilde{\gamma}$ (solid line) in Fig. 12, we obtain the calculated Z^F in Fig. 11 in reasonable agreement with the data. Figure 12 indicates a leveling of the slope of the τ_c versus T curve as the temperature is decreased below 0.2 K. Instead, if the τ_c curve had continued to increase steeply with decreasing T, there would be no measurable damping from fluctuations at 0.1 K, contrary to the observations.

Similar results are obtained for $X = 0.31$, where τ_c has also been determined from longitudinal relaxation times. Here the curves for $\tilde{\gamma}(T)$ and τ_c are found as for $X = 0.46$, but shifted towards lower temperatures to reflect the decrease in the freezing temperature with X.

Having established the existence of a small damping effect from orientational fluctuations, and having for simplicity used an exponential decay of the correlation function, Eq. (33) with $y = 1$, we need to explore the effect of a stretched exponential and we use several values of y smaller than unity and perform a numerical evaluation of Z. This is shown in Fig. 13 for two values of τ_c and for the same value of $\tilde{\gamma}_0$. Over the experimental temperature range, we expect the exponent y to vary from 1 to 0.7, judging from the computer simulations of Binder and Reger.[35] While the shape of the damping function varies with the exponent y, our use of the value $y = 1$ in the calculations of Z is justified because of the crude

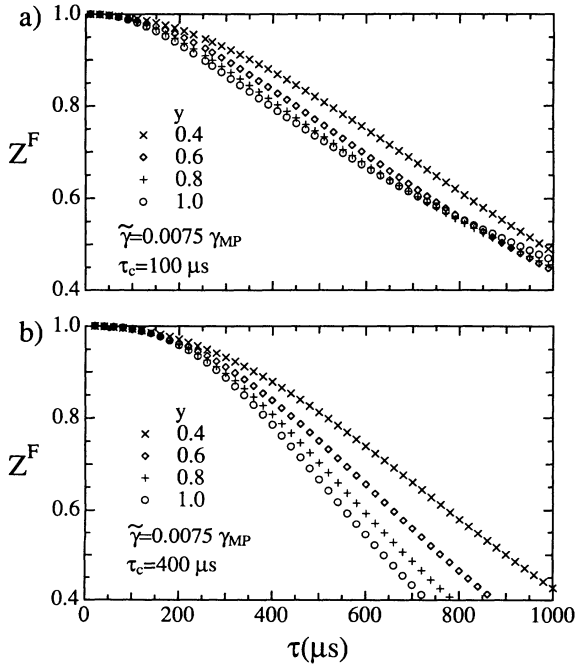

FIG. 13. The calculated Z^F vs τ for various values of the stretch exponent y, and for $\tilde{\gamma} = 0.0075\gamma_{MP}$ and $\tau_c^* = 100$ μs and 400 μs.

approximations we made and because of the uncertainty in the values of τ_c and $\tilde{\gamma}$.

Although the $(I = 1)$ spin system in p-D_2 shows a small but detectable effect from fluctuations, there is no evidence of this in H_2 for a comparable $(J = 1)$ concentration, $X = 0.43$, as seen in Fig. 8 of Ref. 30. We already discussed in Sec. III the expected damping of Z^F from fluctuations and we predicted that it should be much smaller in H_2 than in D_2 simply because the range of τ used in the H_2 experiments is smaller by a factor of 10 than for D_2. Hence the failure to observe this fluctuation driven damping in H_2 is consistent with predictions.

V. SUMMARY

There are several important differences in the properties of solid H_2 and D_2 that have been briefly reviewed. They include the differences (1) in the rate of the $(J = 1)$ to $(J = 0)$ conversion, based on the magnitude of the respective nuclear dipole moments, (2) in the dynamics of the martensitic transition, and (3) in several NMR observations. This paper has focused on this last category that includes (a) the failure to observe a sharp $(I = 1)$ impurity pair spectrum in D_2 while it has been prominently seen and investigated in solid H_2 and (b) the strong departure from Curie's law of the $(I = 1)$ solid echo amplitude, but not that for the $(I = 2)$ spins. For the $(I = 1)$ system, this corresponds to a significant "spin loss," a large fraction of spins that are not "seen," and whose properties therefore cannot be investigated.

We discuss the NMR phenomena as follows.

(a) We suggest that the observation of a structureless Gaussian NMR absorption for $(J = 1)$ pairs in D_2, instead of the predicted spectrum with sharp anisotropic features (as seen in H_2), is caused by the existence of a large crystalline field which is probably random both in its strength and in the orientation of its principal axes. This assumed random distribution may smear out the otherwise sharp lines in the pair spectrum. Evidence is presented that the crystalline field acting on isolated $(J = 1)$ impurities is an order of magnitude larger in D_2 than in H_2. This larger crystalline field attributed to the fact that the density of D_2 is larger than that of H_2.

(b) We develop the first theory of the solid echo amplitude decay as a function of the spacing time τ between the pulses, in which account is taken of the orientational order parameter fluctuations. A closed-form expression is developed as a function of the fluctuation amplitude and the correlation time, assuming an exponential decay of the correlation function. This theory is compared with the observed solid echo amplitude decay in D_2 as a function of τ, leading to an estimate of the fluctuation parameters in the region where progressive orientational ordering of the $(J = 1)$ molecules into a glasslike state is likely to occur. However, the theory is restricted to a range in τ that is covered by experiment, namely, $\tau \geq 30$ μs. It cannot make predictions for very small pulse spacings, where presumably the dramatic signal loss occurs. Therefore this puzzling observation for the $(I = 1)$ signal in solid D_2 in certain regimes of para concentration, which is seen neither for the $(I = 2)$ signal in the same samples nor in solid H_2, remains unexplained.

ACKNOWLEDGMENTS

The authors are indebted to D. Clarkson for his help with solid echo data retrieval and presentation. The research at Duke University has been supported by NSF Low Temperature Physics Grant Nos. DMR 88-20479 and NSF-INT 8820518. A.B.H. was supported in part by the NSF under Grant No. DMR 91-22784.

[1] I. F. Silvera, Rev. Mod. Phys. **52**, 393 (1980).

[2] X. Qin and H. Meyer, Phys. Rev. B **44**, 4165 (1991), and references to earlier work; H. Meyer, Proceedings of the International Conference on Low Temperature Physics LT-20 [Physica B (to be published)].

[3] A. B. Harris, L. I. Amstutz, S. M. Myers, and H. Meyer, Phys. Rev. **175**, 603 (1968).

[4] M. Calkins, R. Banke, X. Li, and H. Meyer, J. Low Temp. Phys. **65**, 47 (1986).

[5] N. S. Sullivan, M. Devoret, B. P. Cowan, and C. Urbina, Phys. Rev. B **17**, 5016 (1978).

[6] A. B. Harris and H. Meyer, Can. J. Phys. **63**, 3 (1985); **64**, 890(E) (1986).

[7] D. Clarkson, X. Qin, and H. Meyer, J. Low Temp. Phys. **91**, 153 (1993).

[8] W. T. Cochran, J. R. Gaines, R. P. McCall, P. E. Sokol, and B. R. Patten, Phys. Rev. Lett. **45**, 1576 (1980).

[9] J. van Kranendonk, *Solid Hydrogen* (Plenum Press, New York, 1983).

[10] H. Meyer, Can. J. Phys. **65**, 1453 (1987).

[11] M. I. Bagatskii, A. I. Krivchikov, V. G. Manzhelii, I. Ya. Minchina, and P. I. Muromtsev, Fiz. Nizk. Temp. **13**, 1001 (1987) [Sov. J. Low Temp. Phys. **13**, 571 (1987)].

[12] R. Banke, X. Li, and H. Meyer, Phys. Rev. B **37**, 7337 (1988).

[13] R. Schweizer, S. Washburn, A. B. Harris, and H. Meyer, J. Low Temp. Phys. **37**, 309 (1979).

[14] A. B. Harris, A. J. Berlinsky, and H. Meyer, Phys. Rev. B **7**, 4720 (1973).

[15] A. B. Harris, Int. J. Quantum Chem. **IIS**, 349 (1968).

[16] A. B. Harris, Phys. Rev. B **1**, 1881 (1970).

[17] X. Li, D. Clarkson, and H. Meyer, Phys. Rev. B **43**, 5719 (1991).

[18] H. Meyer, F. Weinhaus, B. Maraviglia, and R. L. Mills, Phys. Rev. B **6**, 1112 (1972).

[19] R. Schweizer, S. Washburn, and H. Meyer, J. Low Temp. Phys. **37**, 289 (1979).

[20] W. N. Hardy, A. J. Berlinsky, and A. B. Harris, Can. J. Phys. **55**, 1150 (1977).

[21] At low ($J = 1$) concentration in cw experiments, the ($I = 2$) signal is strong and *narrow* and the ($I = 1$) signal from nonisolated molecules is weak and *broad*. Thus cw and echo experiments are complementary. The small ($I = 1$) signal can only be detected by the echo technique where it appears as a sharp spike.

[22] A. B. Harris, Phys. Rev. B **2**, 3495 (1970).

[23] N. F. Ramsey, *Molecular Beams* (Oxford University Press, London, 1956), pp. 235 and 238.

[24] When only the lowest rotational pair doublet energy levels (obtained assuming only EQQ interactions) are thermally populated, the results are as follows. First, when the splitting of the lowest rotational pair doublet, ΔE, is sufficiently large, so that only one of these two levels is thermally occupied, a result of the form of Eq. (4) is obtained, but now with $(3d/8)$ replaced by $(3d/4)$. Second, M_2 for a powder is given by $M_2 = [9d^2/80][1 + 3\tanh^2(\Delta E/k_B T)]$.

[25] In view of the extensive experimental work on solid D_2 (as reviewed in Ref. 1, for instance), it seems unrealistic to assume that the crystalline field energy V_c is large enough to be comparable to the energy splitting 4Γ between the lowest rotational pair doublet and the higher excited pair states. To explain the anomalous broadening of the NMR pair spectrum of solid D_2, it is not sufficient to merely posit the existence of a crystalline field which is larger than that in H_2. Instead, one has to assume that this crystalline field varies randomly from site to site in the orientation of its principal axes and then, no doubt, also in its magnitude. To see this, suppose that the crystalline field has axial symmetry either (a) about the pair axis **n** or (b) about the crystal **c** axis. In case (a) the crystal field would be irrelevant, merely causing a small random variation in the splitting 4Γ. In case (b) one would have to explain why the spectrum of an isolated ($J = 1$) molecule shows no evidence of a NMR splitting and also, for a single crystal sample, shows no dependence on the orientation of the applied magnetic field.

[26] P. Pedroni, M. Chan, R. Schweizer, and H. Meyer, J. Low Temp. Phys. **19**, 537 (1975).

[27] R. J. Roberts, E. Rojas, and J. G. Daunt, J. Low Temp. Phys. **24**, 265 (1976).

[28] S. Washburn, M. Calkins, A. B. Harris, and H. Meyer, J. Low Temp. Phys. **53**, 581 (1983).

[29] X. Qin, D. Clarkson, and H. Meyer, J. Low Temp. Phys. **91**, 119 (1993).

[30] I. Yu, S. Washburn, and H. Meyer, J. Low Temp. Phys. **51**, 369 (1983).

[31] W. N. Hardy and K. W. Gray (unpublished).

[32] W. N. Hardy and A. J. Berlinsky, Phys. Rev. B **8**, 4996 (1986).

[33] M. Calkins, R. Banke, X. Li, and H. Meyer, J. Low Temp. Phys. **65**, 91 (1986).

[34] M. C. Chen and C. P. Slichter, Phys. Rev. B **27**, 278 (1983), and references to earlier spin glass work.

[35] K. Binder and J. D. Reger, Adv. Phys. **41**, 547 (1992), and references therein.